Cerebral Cortex, August 2020;30: 4297–4305

doi: 10.1093/cercor/bhaa008
Advance Access Publication Date: 1 April 2020
Original Article

ORIGINAL ARTICLE

Functional Connectivity of Hippocampal CA3 Predicts Neurocognitive Aging via CA1–Frontal Circuit

Xia Liang[1,2], Li-Ming Hsu[2,3], Hanbing Lu[2], Jessica A. Ash[4], Peter R. Rapp[4] and Yihong Yang[2]

[1]Laboratory for Space Environment and Physical Sciences, Harbin Institute of Technology, Harbin 150001, China, [2]Neuroimaging Research Branch, National Institute on Drug Abuse, Biomedical Research Center, National Institutes of Health (NIH), Baltimore, MD 21224, USA, [3]Department of Radiology and Biomedical Research Imaging Center, University of North Carolina at Chapel Hill, Chapel Hill, NC, 27599, USA, and [4]Laboratory of Behavioral Neuroscience, National Institute on Aging, Biomedical Research Center, NIH, Baltimore, MD 21224, USA

Address correspondence to Peter R. Rapp, Laboratory of Behavioral Neuroscience, National Institute on Aging, Biomedical Research Center, National Institutes of Health (NIH), Baltimore, MD 21224. Email: rappp@mail.nih.gov; Yihong Yang, Neuroimaging Research Branch, National Institute on Drug Abuse, Biomedical Research Center, NIH, Baltimore, MD 21224. Email: yihongyang@intra.nida.nih.gov.

Abstract

The CA3 and CA1 principal cell fields of the hippocampus are vulnerable to aging, and age-related dysfunction in CA3 may be an early seed event closely linked to individual differences in memory decline. However, whether the differential vulnerability of CA3 and CA1 is associated with broader disruption in network-level functional interactions in relation to age-related memory impairment, and more specifically, whether CA3 dysconnectivity contributes to the effects of aging via CA1 network connectivity, has been difficult to test. Here, using resting-state fMRI in a group of aged rats uncontaminated by neurodegenerative disease, aged rats displayed widespread reductions in functional connectivity of CA3 and CA1 fields. Age-related memory deficits were predicted by connectivity between left CA3 and hippocampal circuitry along with connectivity between left CA1 and infralimbic prefrontal cortex. Notably, the effects of CA3 connectivity on memory performance were mediated by CA1 connectivity with prefrontal cortex. We additionally found that spatial learning and memory were associated with functional connectivity changes lateralized to the left CA3 and CA1 divisions. These results provide novel evidence that network-level dysfunction involving interactions of CA3 with CA1 is an early marker of poor cognitive outcome in aging.

Key words: aging, functional connectivity, hippocampus, spatial memory

Introduction

A major aim of neuroscience is to identify how our brain changes as we age. While dementia afflicts about 10% of people over age 65 (Evans et al. 1989), memory deficits are common in healthy older people and can be an early symptom of prodromal neurodegenerative disease. It is thus of great importance to distinguish brain changes associated with normal aging from neuropathological abnormalities indicative of a pathological process. The hippocampus, a structure critical for learning and memory, is among the brain areas most frequently affected in the course of aging (Barnes 1994; Gallagher and Rapp 1997). Comprised of anatomically distinct, but richly interconnected subfields, substantial evidence suggests the principal cell fields of the hippocampus are differentially vulnerable to aging (Small 2001; Small et al. 2004; Burke and Barnes 2006). Studies in rodent and nonhuman primate models demonstrate that, while neural activity patterns are altered in both the CA3 and CA1 pyramidal

cell fields (Barnes et al. 1987, 1992; Barnes 2000; Dieguez and Barea-Rodriguez 2004), the dentate gyrus (DG) and CA3 may be disproportionately affected in relation to age-related memory decline (Small et al. 2004; Wilson 2005; Thomé et al. 2016). These findings have a counterpart in human aging, where high-resolution neuroimaging studies have demonstrated volume loss in normal older adults (Small et al. 2002) and hyperactivity in aMCI restricted to the CA3/DG region (Yassa et al. 2010). Importantly, recent evidence demonstrates that treatments designed to dampen excess CA3 activity improve memory in aged rats (Koh et al. 2010) as well as in patients with aMCI (Bakker et al. 2012). Together, these findings support the concept that age-related dysfunction in CA3 may be an early seed event closely linked to individual differences in memory. What has not been tested, however, is whether the differential vulnerability of CA3 and CA1, in the context of the anatomical organization of the trisynaptic circuit, exhibits broader disruption in network-level functional interactions in relation to age-related memory impairment, and more specifically, whether altered CA3 function contributes to the effects of aging on CA1 network connectivity.

A growing literature points to functional dissociation between the left and right CA3 in memory. In seminal work by Kawakami et al (Kawakami 2003), NR2B expression and the associated capacity for long-term potentiation (LTP) (Lisman et al. 2002) were strongly lateralized, favoring the left, at CA1 dendritic spines that receive presynaptic input from CA3. Related findings indicate that optogenetic stimulation induces greater LTP in CA1 when presynaptic input originates in the left CA3 than the right (Kohl et al. 2011; Shipton et al. 2014). Moreover, while left CA3 silencing impairs performance on a test of spatial associative memory that requires the hippocampus, silencing the right CA3 has no effect (Shipton et al. 2014). These findings suggest an interhemispheric specialization in the rodent hippocampus with a putative left-dominance in long-term memory. The influence of this lateralization on intra- and extrahippocampal network organization, however, particularly in the context of neurocognitive aging, has received limited attention.

To test the hypothesis that CA3 and potential lateralized effects critically regulate cortical network dynamics linked to age-related memory decline, we took advantage of a well-characterized rat model uncontaminated by neurodegenerative disease and optimized for detecting individual differences in the neurocognitive outcome of aging. Animals were scanned under light anesthesia with functional MRI to obtain spontaneous blood oxygenation level-dependent (BOLD) oscillations, and brain-wide functional connectivity of the CA3 and CA1 fields was examined. The results demonstrate that functional connectivity of CA3 and CA1 is widely disrupted in aged rats, such that connectivity between left CA3 and the hippocampal circuit, as well as between the left CA1 and infralimbic (IL) prefrontal area, is significantly coupled with age-related memory impairment. The dysregulated interactions of CA3 and CA1 are left lateralized, with the effects of CA3 connectivity on memory performance mediated by CA1–IL connectivity. These findings suggest an account whereby early reduction of CA3–HPC connectivity may give rise to disrupted CA1–IL connectivity, which in turn underlies age-related decline in episodic learning and memory. The testable implication for intervention is that treatment targeting early CA3 signatures could correct the broader network dysfunction and improve memory outcomes in aging.

Materials and Methods

Animal Preparation

Young adult (Y; 6–8 month; $n = 12$) and aged (24–26 month; $n = 21$) male Long–Evans rats (Charles River Laboratories) were individually housed and maintained under specific pathogen-free conditions on a 12-h light/dark cycle at the National Institute on Aging/National Institute on Drug Abuse (NIA/NIDA) animal facilities in the Biomedical Research Center (Baltimore, MD). Standard rat chow and water were available ad libitum throughout the experiments. Additional subject details are available in our previous reports (Ash et al. 2016; Hsu et al. 2016). This study was approved by the NIA and NIDA Intramural Research Programs' Institutional Animal Care and Use Committees, in accordance with the National Research Council Guide for the Care and Use of Laboratory Animals.

Experimental Design

Animals were first trained in the Morris water maze (MWM) and then transferred to an adjacent vivarium and imaging facilities at NIDA. Hippocampal spatial learning and memory were assessed using a standardized version of the MWM (*SI Materials and Methods*). Spatial memory for each rat was assessed on the basis of a learning index (LI) score, calculated as the weighted average proximity (in centimeters) to the hidden escape location across probe trials (Gallagher et al. 1993). This measure is optimized for identifying reliable individual differences in memory, and was used to classify aged animals as either aged unimpaired (AU), or aged impaired (AI), as described elsewhere (Ash et al. 2016). After an acclimation period of 1 mo, rs-fMRI data were acquired, and repeated only in cases where postacquisition quality-control assessment or physiological monitoring revealed poor data quality from the initial scan.

Image Acquisition

The MRI experiments were performed on a Bruker Biospin 9.4T scanner (Bruker Medizintechnik). High-resolution T2-weighted anatomical images were acquired first, followed by functional MRI scanning (see *supplemental Fig. 1 for exemplar EPI images in each of the three groups*). Animals were anesthetized during scanning using a previously validated protocol combining low-dose medetomidine and isoflurane, optimized for small animal functional neuroimaging studies (Lu et al. 2012). We acquired multiple rs-fMRI scans for each rat, depending on the length of time the animal remained physiologically stable. For detailed anesthesia procedure and acquisition parameters, see *SI Materials and Methods*.

Image Preprocessing

fMRI images were preprocessed using the Analysis of Functional Neuroimaging (AFNI) software package (Cox 1996) and FMRIB Software Library (FSL) (Smith et al. 2004). Detailed preprocessing steps are described in *SI Materials and Methods*.

Seed-Based Functional Connectivity Computation

Seed regions of CA1 and CA3 hippocampal subdivisions were manually drawn on the group-merged T2 anatomical images registered to the common space by identifying their general locale using visualized anatomical landmarks and based chiefly

on the atlas of Paxinos and Watson (2007). CA1 subfield was located using the third ventricle as its medial boundary and the hippocampal fissure as its boundary to the dentate gyrus (DG), and its lateral boundary was limited within 2 mm of the midline between hemispheres. This procedure resulted in a 10-voxel (in fMRI resolution) left CA1 ROI (A-P: −3.36 mm to −4.36 mm) and a 10-voxel right CA1 ROI (A-P: −3.36 mm to −4.36 mm). The CA3 subfield was drawn on the most lateral aspect of the dorsal hippocampus, avoiding overlap with CA2 and the DG, which resulted in a 7-voxel left CA3 ROI (A-P: −3.36 mm to −4.36 mm) and a 7-voxel right CA3 ROI (A-P: −3.36 mm to −4.36 mm). Pearson's correlation coefficients between the mean time course of each seed region and every other voxel in the brain were calculated. To control for potential influence of different number of fMRI scans, for each animal, we only used the two fMRI scans that provide the most robust estimates of functional connectivity. Whole-brain functional connectivity maps for each seed region were constructed by transforming the resulting Pearson correlations using Fisher's r to z, and averaged across the most two robust fMRI scans. These two scans were determined in our previous paper (Ash et al. 2016) using the following procedure. Briefly, we first estimated with-session FC strength between the anterior and posterior hubs of the default mode network (DMN, a network reportedly vulnerable to aging in human studies, Andrews-Hanna et al. 2007). In an effort to extract the most reliable, representative sample of DMN activity, the two scans from each animal that yielded the most similar correlation coefficients were selected for analysis.

Statistics

We used a 3×4 (GROUP × REGION) mixed-design analysis of variance (ANOVA) to compare rsFC maps between the Y, AU, and AI groups. Significance was considered at $P < 0.05$, corrected for multiple comparisons using an uncorrected $P < 0.01$, cluster size = 22 voxels (determined based on Monte Carlo simulations). This ANOVA detected a number of spatially distributed regions showing significant group effects. To assess whether these regions belong to functionally separate brain systems, we conducted graph theory-based modularity analysis to identify modules that refer to groups of nodes that are highly interconnected but less connected with the rest of the network (Newman and Girvan 2004). Details of modularity analysis are described in *SI Materials and Methods*. Modularity analysis that groups the significant voxels as separate modules could also reduce the dimension of predictive variables and promote regression fitting effect in subsequent LASSO analysis.

To explore relationships between spatial learning performance and rsFC within regions of interest resulting from the group-level analysis of variance, we used a LASSO (Least Absolute Shrinkage and Selection Operator) regression analysis as implemented in the freely available GLMNET package in R (Friedman et al. 2015) to select a subset of candidate rsFC predictors. LASSO regression technique is able to evaluate a large number of potential predictors relative to the number of study samples, which is the case for our analysis (28 rsFC predictor variables while only 33 samples for the entire group and 21 samples for aged animals only). LASSO is a modified form of least squares regression that penalizes complex models with a regularization parameter (λ) (Tibshirani 2011). This penalization method shrinks coefficients toward zero, and eliminates unimportant terms entirely (Friedman et al. 2010), thereby minimizing prediction error and overfitting risks. GLMNET uses cross-validation to identify the optimal regularization term λ that would minimize the mean cross validated error for fitted model. For our analysis, we used a k = 10-fold cross validation approach for LASSO model fit across all rats, and a k = 5-fold cross validate for LASSO across aged rats only given the relatively small sample size (21 rats). Learning index scores served as the dependent variable, and mean functional connectivity of brain modules identified from the group-level analysis of variance were independent variables. Results of LASSO fit model across all rats and across only aged rats are displayed in *supplemental Figure 3*.

Results

Neurocognitive Aging Impairs Brain-Wide Functional Interactions of Both CA1 and CA3

During the MWM experiment, young animals exhibited learning (mean ± SEM = 187 ± 8.30, $n = 12$, *supplemental Fig. 4*.) similar to many previous experiments using this model [reviewed in (Fletcher and Rapp 2013)]. Aged rats were categorized based on the normative range of young performance. Those falling within the range of young performance were designated aged unimpaired (mean ± SEM = 208 ± 3.43, $n = 9$), whereas those performing worse than young were considered aged impaired (mean ± SEM = 277 ± 6.74, $n = 12$). Detailed behavioral results are available in our previous work (Ash et al. 2016; Hsu et al. 2016).

Functional connectivity analysis revealed that both CA1 and CA3 exhibited extensive functional interactions with a distributed network of brain regions, prominently including key structures of the rodent hippocampal memory system. Figure 1 displays the areas that are highly connected with CA1 or CA3 seeds in the Y group, including dorsal and ventral hippocampus, dorsal thalamus, retrosplenial cortex, posterior parietal cortex, orbitofrontal, prelimbic and infralimbic prefrontal cortex, anterior cingulate cortex, and primary/secondary auditory and temporal association cortices. Aged rats exhibited a similar anatomical map of functional connectivity, although with less extensive connectivity that reached statistical significance, especially in aged-impaired group.

To explore whether functional connectivity with CA1 and CA3 is altered in the aged rats, we conducted a voxel-wise whole-brain survey in rsFC maps using a mixed-design ANOVA of GROUP and SEED REGION. The results revealed significant main effects of GROUP in extensive brain regions [$F(2,33) > 3.33$, $P < 0.05$, corrected; Fig. 2A]. To further assess the brain systems in which these regions reside, we conducted modularity analysis that allows for topologically dividing nodes in a network into modules. The brain regions with significant group effects were decomposed into seven modules (Fig. 2B), including the bilateral orbitofrontal cortices (OFC), prelimbic (PL) and infralimbic prefrontal cortex (IL), retrosplenial cortex (RSC), right dorsal dentate gyrus/CA1 (rDG/CA1) and the hippocampal complex (HPC) covering dorsal and ventral hippocampus, left temporal association cortex, as well as posterior parietal areas. No significant interaction effect of GROUP by SEED REGION was observed.

Post hoc between-group contrasts showed that the most pronounced age-related changes in hippocampal rsFC occurred in the aged-impaired group. Compared with Y, rsFC of bilateral CA1 regions showed significant and widespread reductions in AI rats, spanning almost all brain structures within the modules noted above (Fig. 2C, $P < 0.05$ corrected). Functional connectivity of CA3 showed similar spatial patterns of reduction in AI animals, with the exception of the decreased or absence of reduction in the

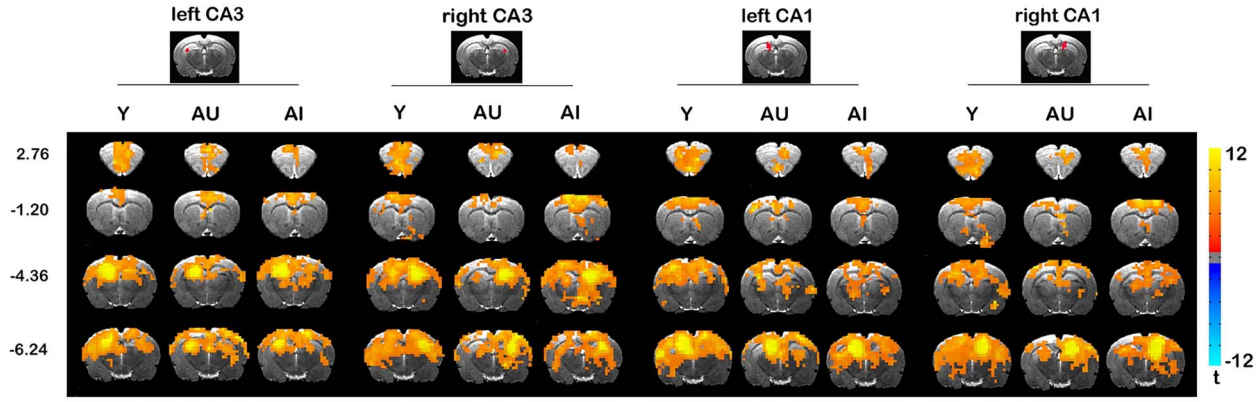

Figure 1. Resting-state functional connectivity maps of left and right CA1 and CA3 hippocampal subdivisions for Y ($n = 12$), AU ($n = 9$), and AI ($n = 12$) rats. $P < 0.05$ by one-sample t-test, corrected for multiple comparisons. Coordinates represent distance relative to bregma (in millimeters).

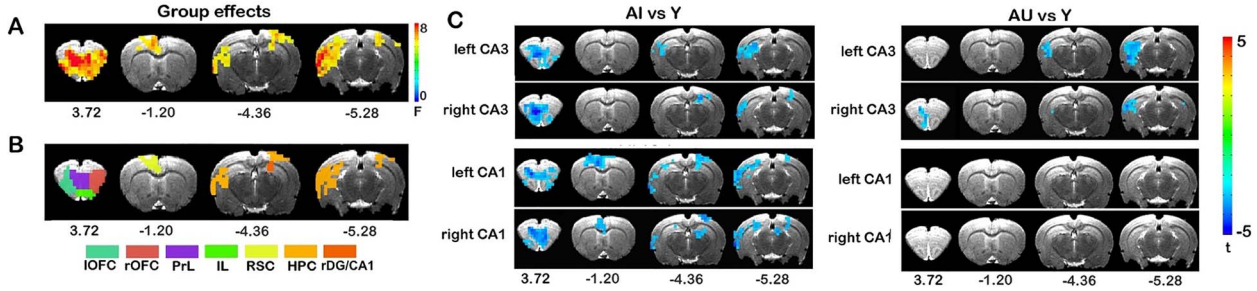

Figure 2. Aging-related alterations in CA1/CA3 connectivity. Mixed-design ANOVA of GROUP (Y, AU and AI) and SEED REGION (left/right CA1 and left/right CA3) revealed brain regions showing significant main effect of group in rsFC of the hippocampal seed region (*A*) are located in seven different modules (*B*). Post hoc contrast maps plotting the distribution of significant differences in rsFC with the CA1/CA3 regions (*C*). $P < 0.05$, corrected for multiple comparisons. Coordinates represent distance relative to bregma (in millimeters).

retrosplenial and posterior parietal cortices. Contrasts between the Y and AU groups revealed a similar but less extensive pattern of reduced rsFC with CA3 (Fig. 2C, $P <$ 0.05 corrected), mostly localized to the prefrontal and ventral hippocampal regions. In contrast, there were no significant alterations in rsFC with CA1 seeds. These findings suggest that age-related decline in functional connectivity with CA3 may precede changes in CA1. We found no significant differences between AU and AI animals in rsFC of any of the CA1 or CA3 seeds.

CA3–HPC Connectivity Drives the Relationship of CA1–IL with Memory in Aging

We next sought to test whether altered functional connectivity of the aged CA1 and CA3 subfields predicts individual differences in spatial learning and memory. We used LASSO analysis to select candidate predictors (rsFC of CA1 and CA3) of spatial learning performance (LI) across animals. Of all the connectivity with bilateral CA regions, LASSO analysis selected two candidate predictors, one connected left CA1 to infralimbic divisions of the prefrontal cortex (LASSO coefficient: −0.066), while the other linked left CA3 to the HPC module (LASSO coefficient: −0.15). Higher LI scores (reflecting poor spatial memory) were predicted by reduced left CA1–IL and left CA3–HPC connectivity, and the LASSO identified model explained 28.5% of the variance in spatial learning performance across all rats.

Given the anatomical organization of hippocampal projections, we suspected that CA3–HPC connectivity might act on the CA1–IL circuit to influence learning and memory. To test this prediction, we conducted a mediation analysis (using the mediation package in *R*, with 10 000 bootstrap samples), in which the predictor variable was left CA3–HPC connectivity, the outcome variable was LI score, and the mediator variable was left CA1–IL connectivity. The results revealed that left CA1–IL connectivity fully mediated the association between left CA3–HPC connectivity and spatial learning index ($\beta = -0.38$; 95% CI, −0.61 to −0.12, $P < 0.01$) (Fig. 3, Table 1); higher connectivity between left CA3 and HPC was associated with better spatial learning ability via increased CA1–IL functional interactions. As a control analysis, we also tested the reverse mediation effect using CA3–HPC rsFC as the mediator for the association between CA1–IL connectivity and learning index. This effect did not approach statistical significance t ($\beta = 0.01$; 95% CI, −0.32 to 0.28; $P = 0.92$; *supplemental Fig. 5*, Table 1).

Since the observed associations and mediation effects might arise predominantly from the between-group differences in FC, we refitted both LASSO and mediation models using the aged rats alone (i.e., both AI and AU rats). LASSO analysis replicated the preceding predictive model using all rats; that is, left CA1–IL (LASSO coefficient: −0.11) and left CA3–HIP rsFC (LASSO coefficient: −0.10) were selected as candidate predictors, which together explained 30.4% of the variance in spatial learning across aged animals. Moreover, the association between CA3–HIP rsFC and learning performance was mediated significantly by CA1–IL connectivity ($\beta = -0.27$; 95% CI, −0.46 to −0.05; $P = 0.04$; supplemental Table 1).

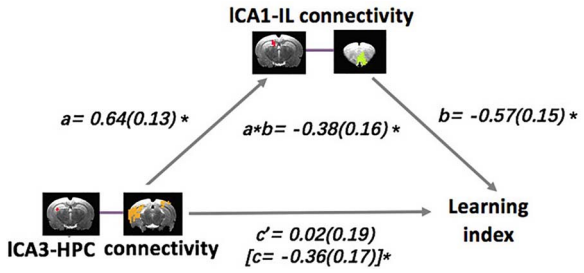

Figure 3. Mediation model for the association between left CA3–HPC connectivity, left CA1–IL connectivity, and learning index, whereby left CA1–IL connectivity is a complete mediator of the relationship between left CA3–HPC connectivity and learning index. Path coefficients are shown next to arrows indicating each link in the analysis, with SEs in parentheses. Path *a* is the relationship between the predictor and the mediator. Path *b* is the relationship between the mediator and the outcome. The total effect (path *c* in square parenthesis) is the relationship between the predictor and the outcome, whereas the direct effect (path *c'*) is the relationship between the predictor and the outcome controlling for the mediator. Path *a***b* is the mediation effect. **P* < 0.05.

Neurocognitive Aging Effects in CA1 and CA3 Are Left Lateralized

Available evidence suggests a left–right dissociation of hippocampal memory processes in rodents, where the left hippocampus may be dominant for spatial long-term memory processing. We therefore sought to assess whether age-related memory decline is associated with lateralized changes in rsFC. Analysis of covariance (ANCOVA) examined the hemisphere × rsFC interaction term to test whether the slopes of the relationship between hippocampal rsFC and LI differed between hemispheres (i.e., using LI scores as the dependent variable, and average rsFC of hippocampal seeds as independent variables). We fitted averaged rsFC between left or right CA1/CA3 seeds and the brain modules with significant group effects in the ANCOVA model, respectively, and observed significant hemisphere × rsFC interactions for associations between LI and CA3–HPC as well as CA1–IL rsFC (supplemental Table 2). Post hoc linear regressions confirmed that LI was significantly correlated with rsFC of both the left CA1 and CA3 fields, but not with the corresponding regions in the right hemisphere (Table 2 and Fig. 4). Similar effects were also observed when the aged rats were considered alone (AI and AU; supplemental Tables 3 and 4).

We also evaluated whether there are laterality effects on neurocognitive aging-related changes in hippocampal connectivity. To do this, we recompared CA1/CA3 rsFC between AI and Y animals after controlling for rsFC with their contralateral seed regions. The comparisons revealed that neurocognitive aging-related reductions in left CA3–HPC rsFC and left CA1–IL rsFC remained significant after regressing out their corresponding contralateral connectivity (i.e., right CA3–HPC rsFC and right CA3–IL rsFC, respectively). In contrast, group differences between AI and Y animals in connectivity with the right hippocampal divisions were no longer significant after controlling for connectivity with left CA1/CA3 areas.

Discussion

In this study, we observed age-related impairments in functional connectivity of both CA3 and CA1, distributed extensively in medial temporal, orbital and medial prefrontal cortices. Age-related deficits in spatial memory were predicted by connectivity between left CA3 and hippocampal circuit along with connectivity between left CA1 and infralimbic area. Importantly, the effects of CA3 connectivity on memory in aging were mediated by CA1–IL connectivity. Moreover, aging-related decline of spatial learning and memory was associated with functional connectivity changes lateralized to the left CA3 and CA1 hippocampal divisions.

Excessive neural activity in the hippocampus is a prominent feature of age-related neurocognitive impairment in both rodents and humans. Recent evidence links hyperactivity selectively in the CA3 subfield with a loss of immunoreactivity for GABAergic interneurons that regulate network inhibition (Thomé et al. 2016). Our findings here suggest that CA3 hyperactivity in aging may arise in association with disrupted network-level communication. Cognitively intact aged animals exhibited reduced functional coupling between the CA3 subfield with regions localized to the prefrontal and ventral hippocampal areas. Previous studies using the same aged rat model reported that cognitively unimpaired subjects maintain normal excitatory/inhibitory balance in the hippocampus (Haberman et al. 2013, 2017), suggesting that subtle changes in functional connectivity with CA3 may comprise an early event, potentially driving eventual changes in activity. Indeed, it has been hypothesized that uncoupling from cortical inputs may lead to disinhibition-like changes in intrahippocampal activity. This disconnection account is supported by recent human studies in patients with AD, showing an inverse relation between hippocampal connectivity and intrahippocampus metabolism (Yakushev et al. 2011; Tahmasian et al. 2015). Our results build significantly on this background, providing evidence that the decline in CA3 connectivity is an early feature of normal aging. However, we note that we cannot rule out the possibility that hyperexcitability of aged hippocampal CA3 may drive further network dysconnectivity. In humans and animals models of neurodegeneration, an "activity-dependent degeneration" model has been proposed that excess neural activity in aging comprises a required permissive condition for the spread of neuropathology, and for consequent network dysconnectivity (Palop and Mucke 2010; de Haan et al. 2012). Although the animals used in the current study will not develop neurodegenerative pathology, we observed that CA3 functional connectivity loss spread from MTL to widely distributed neocortical regions in aged animals with cognitive impairments, indicating hyperactivity may also contribute to further network dysconnectivity and neurocognitive impairments in normal aging. Moreover, the pattern of disrupted functional connectivity we found in AI rats maps out much of the circuity vulnerable to the activity-dependent neurodegenerative processes. Changes in functional connectivity in these networks may be an earlier seed event, or a precursor, providing insight into why aging itself is the greatest risk for neurodegenerative disease. Together, these findings point to a potential feedforward effect whereby CA3 hyperactivity and associated network dysconnectivity reinforce and exacerbate each other.

Although the extent of CA1 dysconnectivity was similar to CA3 in aged-impaired animals, CA1 connectivity was relatively preserved during successfully cognitive aging. These observations are in accordance with previous reports showing differential vulnerability of these two regions, with CA3 being more affected than CA1 in relation to variability in the cognitive outcome of aging (Wilson 2005; Yassa et al. 2010). Using the same model examined here, molecular evidence suggests that spatial

Table 1 Mediation analyses results for the association between left CA3–HPC connectivity, left CA1–IL connectivity, and learning index across all rats

Connectivity/model path	Estimate	95% CI	P-value
Mediator: CA1–IL			
Total effect: direct+mediation effects	−0.36	−0.78 to −0.03	**0.04**
Direct effect: CA3–HIP->LI	0.02	−0.59 to 0.41	0.94
Mediation effect: CA3–HIP->CA1–IL->LI	−0.38	−0.61 to −0.12	<**0.01**
Mediator: CA3–HIP			
Total effect: direct+mediation effects	−0.58	−0.90 to −0.37	<**0.01**
Direct effect: CA1–IL ->LI	−0.59	−0.97 to −0.19	**0.02**
Mediation effect: CA1–IL ->CA3–HIP—> LI	0.01	−0.32 to 0.28	0.92

The total effect is the relationship between the predictor and the outcome, whereas the direct effect is the relationship between the predictor and the outcome controlling for the mediator. Mediation effect is the difference between the total effect and direct effect. Hypothesis testing and statistical significance were evaluated with bootstrapping. An effect was statistically significant if the value 0 was not within the 95% bias-corrected.

learning ability (Haberman et al. 2008) and cognitive status in aged animals (Haberman et al. 2011) are coupled with gene expression changes in CA3, and that among the principal hippocampal subfield, CA3 profiles of differential expression best distinguish aged animals with preserved versus impaired memory (Haberman et al. 2011). Such memory-related differences prominently involve gene expression for inhibitory markers in CA3, consistent with the idea that blunting excess activity in that circuitry is important for intact memory function in the aged hippocampus (Branch et al. 2019). Notably, while functional coupling of both CA3–HPC and CA1–IL were predictive of spatial memory performance, CA1–IL connectivity mediated the effect of CA3–HPC connectivity. These findings suggest that an early reduction in CA3–HPC connectivity may give rise to disrupted CA1–IL connectivity, and that connectivity of CA3–HPC, rather than CA1–IL, may precipitate memory decline during the aging process. The testable implication for intervention is that treatments targeting early CA3 signatures could improve memory performance by circumventing the progression of broader network dysfunction. The mediation effect also offers insight into the neural mechanisms by which dysregulated CA3 connectivity affects spatial learning and memory. The hippocampus and medial prefrontal cortex (mPFC) are strongly connected and the primary projections from the hippocampus to prefrontal cortex originate in the CA1 subdivision (Delatour and Witter 2002). Based on anatomical pathways of different hippocampal subfields, computational models of hippocampal function suggested that the CA3 neurons act as an autoassociative network to form and store episodic memories, which are further recoded by CA1 to enable more efficient recall of activity in the neocortical areas (Kesner and Rolls 2015). The role of mPFC–hippocampal interactions that support memory was updated in a number of recent developments, which suggest that through the direct and indirect CA1–mPFC pathways, contextual information is transferred to the prefrontal cortex, which allows subsequent top-down control by the mPFC in the recall of context-appropriate memory representations stored in the CA3 cells (Eichenbaum 2017). In support of these evidences, our findings of the mediation effect of CA1–IL connectivity suggest its role in coordination with CA3 circuit to facilitate learning and memory performance. However, given the observational nature of the data, it will be important to directly test the sequence of CA3 and CA1 dysconnectivity during neurocognitive aging, and their causal relationship with memory impairment.

While lateralization of function in the human hippocampus is well established, interhemispheric projections are far more extensive in the rodent brain (Amaral and Lavenex 2006), directly impacting the anatomical organization presumed to mediate functional asymmetries. It is only recently that advanced technologies, such as optogenetics, have uncovered evidence suggesting that the left and right rodent hippocampi are also functionally specialized (Kohl et al. 2011; Shipton et al. 2014). Here, using an aging model in rats, we report that aging-related memory decline is associated with functional connectivity changes lateralized to the left hippocampus. Indeed, earlier work points to a potential interaction between aging and lateralization, demonstrating that unilateral hippocampal inactivation selectively impairs spatial memory in aged rats when the left hippocampus is inactivated (Poe et al. 2000). It is interesting to note in this context that aging-related disruptions in hippocampal integrity reported in human studies often appear localized in the left hemisphere (Yassa et al. 2011; Reagh et al. 2018). Whether lateralization contributes to the differential vulnerability of different forms of memory to aging remains to be tested directly.

The findings from the present study should be interpreted in view of a few limitations. First, functional connectivity analysis was performed using fMRI BOLD signal, which reflects neural activity indirectly based on vascular responses. Evidence from human aging studies has shown that vasodilatory capacity declines with age (Ito et al. 2002; Lu et al. 2011), which may manifest as a plausible cause of aging-related fMRI differences (Lu et al. 2013). Thus, future studies should investigate the vascular origin of functional connectivity changes during neurocognitive aging by using cerebrovascular reactivity-corrected BOLD fMRI data. Second, although general physiology including arterial oxygen concentration, cardiac and respiration rates were monitored and maintained in the normal physiological range during scanning in our study, there was still a marginal difference in respiration rate between the aged subgroups (AI vs. AU: Mann–Whitney test, $U = 38$, $P = 0.053$). To control for potential contamination of respiration circle on connectivity measures, we specifically removed respiration-related components during preprocessing of fMRI data (see section "Materials and Methods"). Moreover, our previous observation that no significant differences were observed in rsFC with a piriform cortex seed suggests that age-related changes in general physiology are unlikely to account for the selective pattern of results we observed (Ash et al. 2016). Nevertheless, future studies using mechanical

Table 2 Hemisphere × Connectivity Interaction Effects for Associations Between LI and CA3–HPC/CA1–IL Connectivity Across only Aged Rats

y	x	Hemisphere	Regression parameters		ANCOVA	
			β(SE)	P	F	P
LI	**CA3–HPC connectivity**	left CA3	**−0.47(0.16)**	**0.006**	**11.16**	**0.0014**
		right CA3	0.30(0.17)	0.10		
LI	**CA1–IL connectivity**	left CA1	**−0.41(0.16)**	**0.02**	**4.92**	**0.03**
		right CA1	0.10(0.18)	0.57		

Analysis of covariance (ANCOVA) was used to determine if slopes differed statistically between hemispheres. Statistically significant regression slopes and slope differences between treatments (at $P < 0.05$) are in bold type.

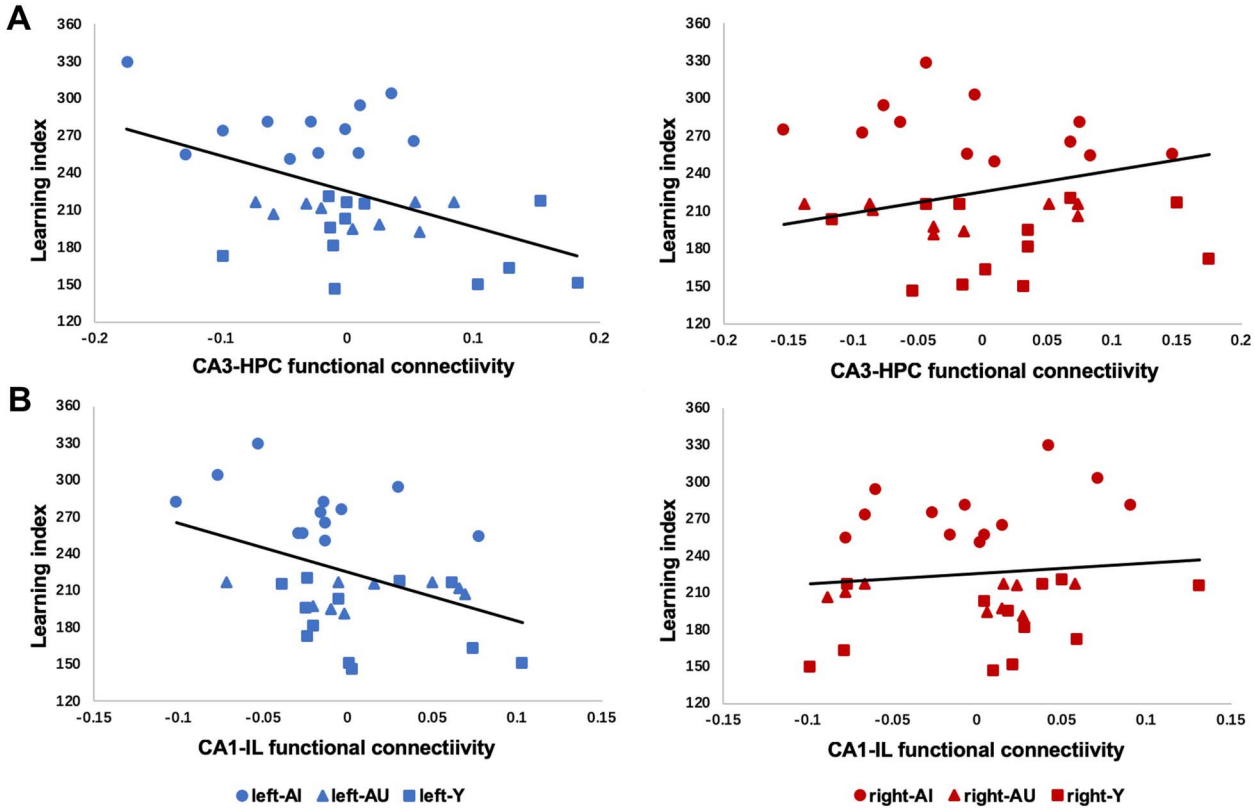

Figure 4. Hemisphere×connectivity interaction effects for associations between LI and CA3–HPC/CA1–IL connectivity. (*A*) Scatterplots of the correlation between CA3–HPC connectivity and spatial memory (LI score) for all rats ($n = 33$). Left CA3–HPC connectivity was significantly negatively correlated with LI score (left panel, $r = -0.47$, $P = 0.006$), while right CA3–HPC connectivity was not (right panel, $r = 0.30$, $P = 0.10$); (*B*) scatterplots of the correlation between CA1–IL connectivity and LI score for all rats ($n = 33$). Left CA1–IL connectivity was significantly negatively correlated with LI score (left panel, $r = -0.41$, $P = 0.02$), while right CA1–IL connectivity was not (right panel, $r = 0.10$, $P = 0.57$).

ventilation would be insightful to reveal if there is a dependence on systemic physiological parameters. Finally, although previous quantitative morphometric studies of post-mortem histological preparations in the same model used here have uniformly failed to detect evidence of gross neuroanatomical change of the sort likely to affect regional brain volumes (e.g., Rapp and Gallagher 1996; Smith et al. 2000; Rapp et al. 2002), it is plausible future morphometric analysis may reveal neurocognitive aging-related changes and their relationship with functional dysconnectivity of hippocampal subfields.

In conclusion, the current study reveals that CA3, the hippocampal subdivision most vulnerable to aging, is characterized by dysregulated functional network connectivity lateralized to the left hippocampi, and, through the left lateralized dysconnectivity within the CA1–mPFC circuit, provides a network mechanism for learning and memory impairment in aging.

Supplementary Material

Supplementary material can be found at *Cerebral Cortex* online.

Funding

This research was supported by the Natural Science Foundation of China (Grant No. 81671769), the Intramural Research Programs of the National Institute on Drug Abuse and the National Institute on Aging, National Institutes of Health, the Fundamental

Research Funds for the Central Universities of China (Grant No. HIT. NSRIF. 2020042), and the Natural Science Foundation of Heilongjiang Province, China (Grant No. LH2019H001).

Notes

Author Contributions: XL, PRR, JAA, and YY designed the research. LMH, JAA, and HL collected the data. XL and HL analyzed the data. XL, PRP, and YY wrote the manuscript. Address correspondence to Peter R. Rapp, Email: rappp@mail.nih.gov; Yihong Yang, Email: yihongyang@intra.nida.nih.gov. *Conflict of Interest:* The authors declare no conflict of interest.

References

Andrews-Hanna JR, Snyder AZ, Vincent JL, Lustig C, Head D, Raichle ME, Buckner RL. 2007. Disruption of large-scale brain systems in advance aging. *Neuron*. 56:924–935.

Amaral DG, Lavenex P. 2006. Hippocampal neuroanatomy. In: *The Hippocampus Book*. Oxford Scholarship.

Ash JA, Lu H, Taxier LR, Long JM, Yang Y, Stein EA, Rapp PR. 2016. Functional connectivity with the retrosplenial cortex predicts cognitive aging in rats. *Proc Natl Acad Sci*. 113:12286–12291.

Bakker A, Krauss GL, Albert MS, Speck CL, Jones LR, Stark CE, Yassa MA, Bassett SS, Shelton AL, Gallagher M. 2012. Reduction of hippocampal hyperactivity improves cognition in amnestic mild cognitive impairment. *Neuron*. 74:467–474.

Barnes CA. 1994. Normal aging: regionally specific changes in hippocampal synaptic transmission. *Trends Neurosci*. 17:13–18.

Barnes CA. 2000. LTP induction threshold change in old rats at the perforant path-granule cell synapse. *Neurobiol Aging*. 21:613–620.

Barnes CA, Rao G, Foster TC, McNaughton BL. 1992. Region-specific age effects on AMPA sensitivity: electrophysiological evidence for loss of synaptic contacts in hippocampal field CA1. *Hippocampus*. 2:457–468.

Barnes CA, Rao G, McNaughton BL. 1987. Increased electrotonic coupling in aged rat hippocampus: a possible mechanism for cellular excitability changes. *J Comp Neurol*. 259:549–558.

Branch A, Monasterio A, Blair G, Knierim JJ, Gallagher M, Haberman RP. 2019. Aged rats with preserved memory dynamically recruit hippocampal inhibition in a local/global cue mismatch environment. *Neurobiology Aging*. 76:151–161.

Burke SN, Barnes CA. 2006. Neural plasticity in the ageing brain. *Nat Rev Neurosci*. 7:30–40.

Cox RW. 1996. AFNI: software for analysis and visualization of functional magnetic resonance Neuroimages. *Comput Biomed Res*. 29:162–173.

de Haan W, Mott K, van Straaten ECW, Scheltens P, Stam CJ. 2012. Activity dependent degeneration explains hub vulnerability in Alzheimer's disease. *PLoS Comput Biol*. 8:e1002582.

Delatour B, Witter MP. 2002. Projections from the parahippocampal region to the prefrontal cortex in the rat: evidence of multiple pathways. *Eur J Neurosci*. 15:1400–1407.

Dieguez D, Barea-Rodriguez EJ. 2004. Aging impairs the late phase of long-term potentiation at the medial perforant path-CA3 synapse in awake rats. *Synapse*. 52:53–61.

Eichenbaum H. 2017. Prefrontal–hippocampal interactions in episodic memory. *Nat Rev Neurosci*. 18:547–558.

Evans DA, Funkenstein HH, Albert MS, Scherr PA, Cook NR, Chown MJ, Hebert LE, Hennekens CH, Taylor JO. 1989. Prevalence of Alzheimer's disease in a community population of older persons. Higher than previously reported. *JAMA*. 262:2551–2556.

Fletcher BR, Rapp RP. 2013. Normal Neurocognitive Aging. In: Weiner IB, Nelson RJ, Mizumori S, editors. *Handbook of Psychology, 2nd Edition, Vol. 3: Biological Psychology and Neuroscience*. Hoboken, NJ: Wiley & Sons, Inc., pp. 643–664.

Friedman AJ, Hastie T, Simon N, Tibshirani R, Hastie MT. 2015. Lasso and elastic-net regularized generalized linear models. Available online https://cran.r-project.org/web/packages/glmnet/glmnet.pdf (Verified 29 July 2015).

Friedman J, Hastie T, Tibshirani R. 2010. Regularization paths for generalized linear models via coordinate descent. *J Stat Softw*. 33.

Gallagher M, Burwell R, Burchinal M. 1993. Severity of spatial learning impairment in aging: Development of a learning index for performance in the Morris water maze. *Behav Neurosci*. 107(4):618–626.

Gallagher M, Rapp PR. 1997. The use of animal models to study the effects of aging on cognition. *Annu Rev Psychol*. 48:339–370.

Haberman RP, Lee HJ, Colantuoni C, Koh MT, Gallagher M. 2008. Rapid encoding of new information alters the profile of plasticity-related mRNA transcripts in the hippocampal CA3 region. *Proc Natl Acad Sci*. 105:10601–10606.

Haberman RP, Colantuoni C, Stocker AM, Schmidt AC, Pedersen JT, Gallagher M. 2011. Prominent hippocampal CA3 gene expression profile in neurocognitive aging. *Neurobiology of Aging*. 32:1678–1692.

Haberman RP, Colantuoni C, Koh MT, Gallagher M. 2013. Behaviorally activated mRNA expression profiles produce signatures of learning and enhanced inhibition in aged rats with preserved memory. *PLoS One*. 8:e83674.

Haberman RP, Koh MT, Gallagher M. 2017. Heightened cortical excitability in aged rodents with memory impairment. *Neurobiol Aging*. 54:144–151.

Hsu L-M, Liang X, Gu H, Brynildsen JK, Stark JA, Ash JA, Lin C-P, Lu H, Rapp PR, Stein EA *et al*. 2016. Constituents and functional implications of the rat default mode network. *Proc Natl Acad Sci*. 113:E4541–E4547.

Ito H, Kanno I, Ibaraki M, Hatazawa J. 2002. Effect of aging on cerebral vascular response to Paco2 changes in humans as measured by positron emission tomography. *J Cereb Blood Flow Metab*. 22:997–1003.

Kawakami R. 2003. Asymmetrical allocation of NMDA receptor epsilon2 subunits in hippocampal circuitry. *Science*. 300:990–994.

Kesner RP, Rolls ETA. 2015. Computational theory of hippocampal function, and tests of the theory: new developments. *Neurosci Biobehav Rev*. 48:92–147.

Koh MT, Haberman RP, Foti S, McCown TJ, Gallagher M. 2010. Treatment strategies targeting excess hippocampal activity benefit aged rats with cognitive impairment. *Neuropsychopharmacology*. 35:1016–1025.

Kohl MM, Shipton OA, Deacon RM, Rawlins JNP, Deisseroth K, Paulsen O. 2011. Hemisphere-specific optogenetic stimulation reveals left-right asymmetry of hippocampal plasticity. *Nat Neurosci*. 14:1413–1415.

Lisman J, Schulman H, Cline H. 2002. The molecular basis of CaMKII function in synaptic and behavioural memory. *Nat Rev Neurosci*. 3:175–190.

Liu P, Hebrank CH, Rodrigue MR, Kennedy MK, Section J, Park CP, Lu H. 2013. Age-related differences in memory-encoding fMRI

responses after accounting for decline in vascular reactivity. *NeuroImage*. 78:415–425.

Lu H, Xu F, Rodrigue KM, Kennedy KM, Cheng Y, Flicker B, Hebrank AC, Uh J, Park DC. 2011. Alterations in cerebral metabolic rate and blood supply across the adult lifespan. *Cereb Cortex*. 21:1426–1434.

Lu H, Zou Q, Gu H, Raichle ME, Stein E, Yang Y. 2012. Rat brains also have a default mode network. *Proc Natl Acad Sci*. 109:3979–3984.

Newman MEJ, Girvan M. 2004. Finding and evaluating community structure in networks. *Phys Rev E*. 69:026113.

Palop JJ, Mucke L. 2010. Amyloid-β–induced neuronal dysfunction in Alzheimer's disease: from synapses toward neural networks. *Nat Neurosci*. 13:812–818.

Paxinos G, Watson C. 2007. The rat brain in stereotaxic coordinates. New York, NY: Academic Press.

Poe GR, Teed RGW, Insel N, White R, McNaughton BL, Barnes CA. 2000. Partial hippocampal inactivation: effects on spatial memory performance in aged and young rats. *Behav Neurosci*. 114:940–949.

Rapp PR, Gallagher M. 1996. Preserved neuron number in the hippocampus of aged rats with spatial learning deficits. *Proc Natl Acad Sci*. 93:9926–9930.

Rapp PR, Deroche PS, Mao Y, Burwell RD. 2002. Neuron number in the parahippocampal region is preserved in aged rats with spatial learning deficits. *Cerebral Cortex*. 12:1171–1179.

Reagh ZM, Noche JA, Tustison NJ, Delisle D, Murray EA, Yassa MA. 2018. Functional imbalance of anterolateral Entorhinal cortex and hippocampal dentate/CA3 underlies age-related object pattern separation deficits. *Neuron*. 97. e4: 1187–1198.

Shipton OA, El-Gaby M, Apergis-Schoute J, Deisseroth K, Bannerman DM, Paulsen O, Kohl MM. 2014. Left–right dissociation of hippocampal memory processes in mice. *Proc Natl Acad Sci*. 111:15238–15243.

Small SA. 2001. Age-related memory decline. *Arch Neurol*. 58:360–364.

Small SA, Chawla MK, Buonocore M, Rapp PR, Barnes CA. 2004. Imaging correlates of brain function in monkeys and rats isolates a hippocampal subregion differentially vulnerable to aging. *Proc Natl Acad Sci*. 101:7181–7186.

Small SA, Tsai WY, DeLaPaz R, Mayeux R, Stern Y. 2002. Imaging hippocampal function across the human life span: is memory decline normal or not? *Ann Neurol*. 51:290–295.

Smith SM, Jenkinson M, Woolrich MW, Beckmann CF, Behrens TEJ, Johansen-Berg H, Bannister PR, De Luca M, Drobnjak I, Flitney DE *et al*. 2004. Advances in functional and structural MR image analysis and implementation as FSL. *Neuroimage*. 23:S208–S219.

Smith TD, Adams MM, Gallagher M, Morrison JH, Rapp PR. 2000. Circuit-specific alterations in synaptophysin immunoreactivity predict spatial learning impairment in aged rats. *J. Neurosci*. 20:6587–6593.

Tahmasian M, Pasquini L, Scherr M, Meng C, Forster S, Mulej Bratec S, Shi K, Yakushev I, Schwaiger M, Grimmer T *et al*. 2015. The lower hippocampus global connectivity, the higher its local metabolism in Alzheimer disease. *Neurology*. 84:1956–1963.

Thomé A, Gray DT, Erickson CA, Lipa P, Barnes CA. 2016. Memory impairment in aged primates is associated with region-specific network dysfunction. *Mol Psychiatry*. 21:1257–1262.

Tibshirani R. 2011. Regression shrinkage and selection via the lasso: a retrospective. *J R Stat Soc Ser B (Statistical Methodol)*. 73:273–282.

Wilson IA. 2005. Age-associated alterations of hippocampal place cells are subregion specific. *J Neurosci*. 25:6877–6886.

Yakushev I, Schreckenberger M, Müller MJ, Schermuly I, Cumming P, Stoeter P, Gerhard A, Fellgiebel A. 2011. Functional implications of hippocampal degeneration in early Alzheimer's disease: a combined DTI and PET study. *Eur J Nucl Med Mol Imaging*. 38:2219–2227.

Yassa MA, Mattfeld AT, Stark SM, Stark CEL. 2011. Age-related memory deficits linked to circuit-specific disruptions in the hippocampus. *Proc Natl Acad Sci*. 108:8873–8878.

Yassa MA, Stark SM, Bakker A, Albert MS, Gallagher M, Stark CEL. 2010. High-resolution structural and functional MRI of hippocampal CA3 and dentate gyrus in patients with amnestic mild cognitive impairment. *Neuroimage*. 51:1242–1252.